CuI/CuII Chiral Homoleptic Complexes: Study of Self-Recognition and Self-Discrimination

Caitlyn Dussart, Stéphane Bellemin-laponnaz, Antoine Bonnefont

EurJIC
European Journal of Inorganic Chemistry

Research Article
doi.org/10.1002/ejic.202400527

Chemistry Europe
European Chemical Societies Publishing

www.eurjic.org

Cu^{I}/Cu^{II} Chiral Homoleptic Complexes: Study of Self-Recognition and Self-Discrimination

Caitlyn Dussart,[a] Antoine Bonnefont,[b] and Stéphane Bellemin-Laponnaz*[a]

The formation of ML_2 homoleptic copper(I) and copper(II) complexes from bidentate chiral ligands with C_2 symmetry, comprising three types of substituents (namely benzyl, indanyl and phenyl groups), was investigated. The formation of homochiral or heterochiral complexes can be influenced by the nature of the substituents and the geometry induced by the oxidation state of the metal. All the complexes were isolated and characterized, in particular in the solid state by X-ray diffraction studies. In solution, cyclic voltammetry was used to study ligand association and discrimination induced by the Cu^{I}/Cu^{II} transition.

Introduction

The phenomena of intermolecular assembly are an important area of study in molecular chirality. The fundamental functions of recognition and replication in biological world are made possible by non-covalent interactions between chiral entities.[1] In recent years, we have been focusing on chiral recognition in transition metal complexes.[2] The association of two equivalents of a chiral ligand around a transition metal to give an ML_2-type complex leads to the possible formation of two diastereoisomers, i.e. self-discrimination or self-recognition depending on the geometry of metal.[3–5]

Recently, we have shown that the chiral C_2-symmetric valinol-based bisoxazoline ligand (i.e. *i*Pr substituents) led to the formation of heterochiral complexes in a tetrahedral metal environment and, on the other hand, to the formation of homochiral species in a square planar environment. This allowed us to *in situ* observe that chiral self-recognition or self-discrimination may be induced by the Cu^{I}/Cu^{II} redox transition using cyclic voltammetry.[6,7] We then attempted to synthesize and characterize all the complexes at both oxidation states, but were unable to isolate the copper(I) complexes, which proved too sensitive. Since steric constraint around copper(I) in $[Cu(L)_2]^+$ complexes, where L is a diimine ligand, is known to be a parameter of the stability of the entity,[8,9] we explored a way of improving the stability of copper(I) by playing on more bulky substituents on bisoxazoline ligands.

Herein, we have synthesized a complete series of homoleptic copper(I) and copper(II) complexes stabilized by chiral bisoxazoline BOX ligands all containing phenyl rings, i.e. benzyl, indanyl or phenyl substituents, labeled BOX-Bn, BOX-Ind and BOX-Ph respectively (Figure 1).[10,11] Interestingly, in all cases, the copper(I) complexes proved stable enough to be characterized, in particular by NMR. The systems were also studied in solution in order to evaluate their ligand rearrangements by Cu^{I}/Cu^{II} redox change using cyclic voltammetry. This shows that the ligand substituent change has a significant impact on the associated chiral coordination chemistry, and that steric constraint is not the only parameter to be considered in these systems.

Results and Discussion

Coordination Chemistry with BOX-Bn Ligands

We first investigated the coordination chemistry of BOX-Bn with Cu(II), i.e. $Cu(BF_4)_2$. Two equivalents of ligand, in racemic or enantiopure form, and one equivalent of copper salt were stirred in MeOH for 30 minutes. After removing the solvent, the turquoise solid obtained was dissolved in dichloromethane and slow diffusion of *n*-pentane into the solution gave blue crystals in high yield in both cases, which were suitable for X-ray analysis.

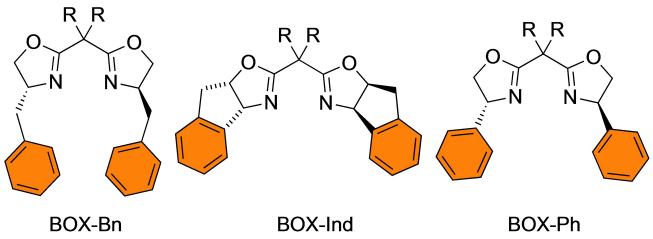

Figure 1. General molecular structure of the bisoxazoline used in the study.

[a] C. Dussart, S. Bellemin-Laponnaz
IPCMS, Institut de Physique et Chimie des Matériaux de Strasbourg, Université de Strasbourg-CNRS UMR 7504, 23 rue du Loess, BP 43, 67034 Strasbourg Cedex 2, France
E-mail: bellemin@unistra.fr

[b] A. Bonnefont
LEPMI, UMR 5279 CNRS-Université Grenoble Alpes, Université Savoie Mont Blanc, 1130 Rue de la Piscine, 38610 Gières, France

Supporting information for this article is available on the WWW under https://doi.org/10.1002/ejic.202400527

Research Article
doi.org/10.1002/ejic.202400527

Analyses revealed the formation of the monoligated complex [(BOX-Bn)$Cu^{II}F(H_2O)$][BF_4] (**1**) in both cases (eq. 1). Figure 2 displays the molecular structure obtained starting from the (*R*)-BOX-Bn. Complex (**1**) was crystallized in the triclinic P_1 space group. The geometry around the metal is distorted octahedral, with bond distances and angles within the range of such type of complex.[12] The coordination sphere of the copper centre is stabilized apically by BF_4^- counterions, forming a coordination polymer. Each counter-ion is shared with another copper(II) complex. Complex (**1**) obtained from racemic BOX-Bn was crystallized in the monoclinic centrosymmetric $P2_1/n$ space group (see ESI and Figure S1 for details). We have tried to detect the presence of homoleptic complexes ML_2, in particular by studies by *in situ* mass spectrometry, but these studies proved unsuccessful.

$$2\ \text{BOX-Bn} + [Cu^{II}(BF_4)_2] \longrightarrow [(\text{BOX-Bn})Cu^{II}F(H_2O)]^+ \quad (1)$$
enantiopure or racemic

We then investigated the coordination chemistry starting from copper(I). Under argon, two equivalents of BOX-Bn, in racemic or enantiopure form, were reacted with one equivalent $(CH_3CN)_4Cu(BF_4)$ in dichloromethane.

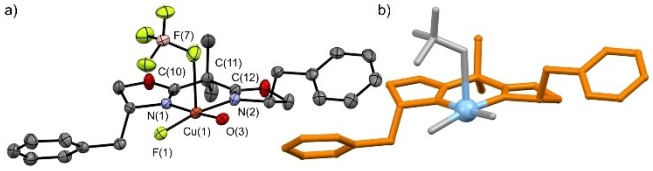

Figure 2. Molecular structure of [{(*R*)-BOX-Bn}$Cu^{II}F(H_2O)$][BF_4] (1): a) ORTEP view. Hydrogens are omitted for clarity. Selected bond lengths (Å) and angles (°): Cu–N(1) 1.971(3); Cu–N(2) 1.952(3); O(3)–Cu(1) 1.965(3); Cu(1)–F(1) 1.896(2); Cu(1)–F(7) 2.546(7); C(10)–C(11)–C(12) 112.8(3); N(2)–Cu(1)–N(1) 91.21(13). (b) Molecular structure of the complex with (*R*)-BOX-Bn in orange.

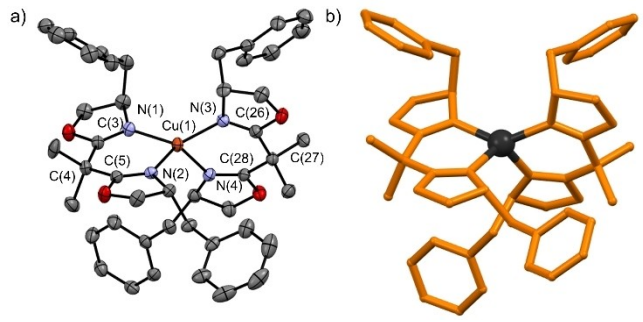

Figure 3. Molecular structure of [Cu^{I}{(*R*)-BOX-Bn}$_2$][BF_4] (2): a) ORTEP view. Hydrogens and BF_4^- counter-ion are omitted for clarity. Selected bond lengths (Å) and angles (°): Cu–N(1) 1.998(4); Cu–N(2) 2.059(4); Cu–N(3) 2.010(3); Cu–N(4) 2.043(3); C(3)–N(1) 1.263(6); C(3)–C(4)–C(5) 113.2(4); C(26)–C(27)–C(28) 112.7(4); N(1)–Cu–N(2) 90.05(16); N(3)–Cu–N(4) 89.40(16); N(1)–Cu–N(3) 137.77(17); N(1)–Cu–N(4) 114.64(17); N(3)–Cu–N(2) 110.03(17); N(4)–Cu–N(2) 117.09(16). (b) Molecular structure of the complex with (*R*)-BOX-Bn in orange.

$$2\ \text{BOX-Bn} + [(CH_3CN)_4Cu^{I}(BF_4)] \longrightarrow [Cu^{I}(\text{BOX-Bn})_2]^+ \quad (2)$$
enantiopure or racemic — *homochiral*

Starting from (*R*)-BOX-Bn, a homoleptic ML_2 complex [Cu^{I}{(*R*)-BOX-Bn}$_2$][BF_4] (**2**) was isolated in 74% yield after recrystallisation (eq. 2). The complex was found stable under air. Figure 3 displays the molecular structure along with selected bond lengths and angles. Complex (**2**) has a distorted tetrahedral geometry ($\tau_4 = 0.75$). This calculated geometry index τ_4 can quantitatively describe the geometry adopted by four-coordinate complexes, according to Houser *et al.*[13] The values of τ_4 range are from 1.00 for a perfect tetrahedral geometry to 0.00 for a perfect square plane geometry. The Cu–N bond lengths range from 1.998 to 2.059 Å, which is typical for this type of compound.[11,12,14–17] Because of the free rotation given by the CH_2 group, the phenyl groups are oriented away from each other, which limits steric interactions between them.

Starting from (*rac*)-BOX-Bn, a homoleptic ML_2 complex [Cu^{I}(−BOX-Bn$_2$][BF_4] (**2**) was also isolated in 75% yield. Unlike the previous one, we did not manage to obtain any crystals. Since mass spectrometry and elemental analysis are unable to determine whether homochiral or heterochiral species have been formed, we conducted NMR studies. Figure S2 shows the proton spectra of the free ligand, as well as the complex homochiral complex [Cu^{I}{(*R*)-BOX-Bn}$_2$][BF_4] obtained previously and the complex obtained from (*rac*)-BOX-Bn. The study shows that the two complexes have the same spectral signature, suggesting that homochiral complexes are formed in both cases.

Coordination Chemistry with BOX-Ind Ligands

The BOX-Ind ligand was studied under the same conditions as with BOX-Bn (eq. 3). Starting from (*R*)-BOX-Ind, a homoleptic copper(II) complex was formed, which could be isolated as a green solid in 89% yield. Crystals of [Cu^{II}{(*R*)-BOX-Ind}$_2$][BF_4]$_2$ (**3**) suitable for X-ray diffraction studies were successfully obtained and the molecular structure was established (Figures 4a and b). The copper(II) cation has a highly distorted geometry between square-planar and tetrahedral geometry ($\tau_4 = 0.55$). The Cu–N bond lengths are ranging in typical values.[11,12,14–17] We also conducted CD measurements in solution, mirror-image spectra being obtained for the two enantiomers as shown on Figure 4c. They show an intense band peaking at 260 nm, two bands at 306 and 348 nm and an intense band at 659 nm arising from d-d transition bands.

$$2\ \text{BOX-Ind} + [Cu^{II}(BF_4)_2] \longrightarrow [Cu^{II}(\text{BOX-Ind})_2]^{2+} \quad (3)$$
enantiopure — *homochiral*

Interestingly, the preparation of the same complex but starting from the racemic mixture of the ligand resulted in the formation of two types of crystals after recrystallisation, green and blue (eq. 4). The X-ray analysis of the green crystals revealed the presence of the racemic mixture of homochiral

Research Article
doi.org/10.1002/ejic.202400527

Chemistry Europe
European Chemical Societies Publishing

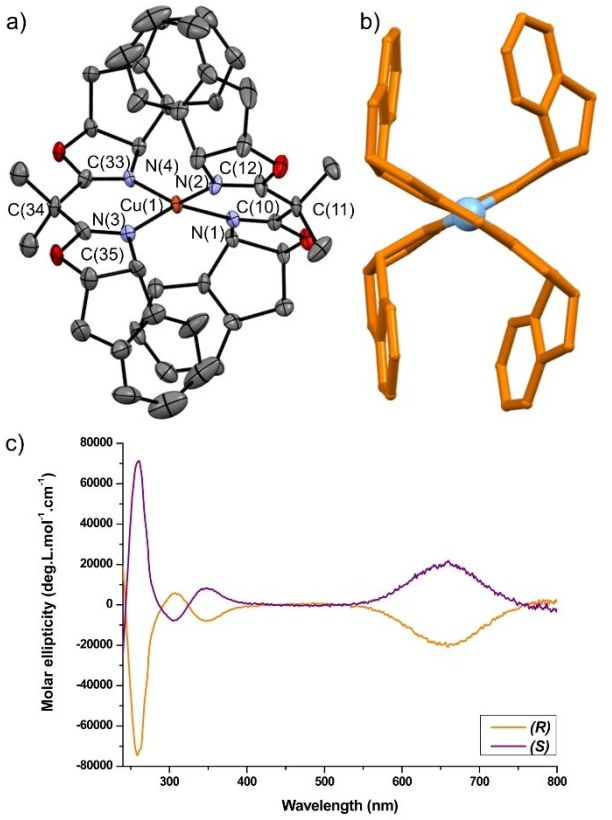

Figure 4. Molecular structure of $[Cu^{II}\{(R)\text{-BOX-Ind}\}_2][BF_4]_2$ (3): a) ORTEP view. Hydrogens and BF_4^- counter-ions are omitted for clarity. Selected bond lengths (Å) and angles (°): Cu–N(1) 1.996(6); Cu–N(2) 1.942(7); Cu–N(3) 1.949(7); Cu–N(4) 1.984(7); N–Cu–N: N(1)–Cu–N(2) 91.9(3); N(3)–Cu–N(4) 91.5(3); N(2)–Cu–N(3) 95.8(2); N(2)–Cu–N(4) 140.3(3); N(3)–Cu–N(1) 142.5(3); N(4)–Cu–N(1) 105.4(2). (b) Molecular structure of the complex with (*R*)-BOX-Ind in orange (methyl groups are omitted for clarity). c) Circular dichroism of the two enantiomers of (3) ($c = 2.96.10^{-4}$ M in dichloromethane).

species (**3**) (Figure S3). While the enantiopure complex was crystallized in the C2 monoclinic space group, the racemate was obtained in the monoclinic C2/c space group. The X-ray analysis of the blue crystals revealed the presence of a heteroleptic dimeric complex $[(BOX\text{-}Ind)Cu^{II}F]_2[BF_4]_2$ (**4**) (Figure 5). The copper(II) centre has a square pyramidal geometry, stabilized by a fluorine atom of the BF_4- counter-ion in the apical position. The torsion angle between the bisoxazoline ligands is 0°, showing that all the atoms involved in the first copper coordinate sphere are in the same plane. This observation is also highlighted by the angle involving the ligands and the copper cation, close to 90° for each F–Cu-F, N–Cu-F and N–Cu-N angle.

$$\underset{\textit{racemic}}{2\ BOX\text{-}Ind + [Cu^{II}(BF_4)_2]} \longrightarrow \begin{array}{c}[Cu^{II}(BOX\text{-}Ind)_2]^{2+}\\ \textit{homochiral}\\ +\\ [\{(BOX\text{-}Ind)Cu^{II}F\}_2]^{2+}\\ \textit{heterochiral}\end{array} \quad (4)$$

Turning our attention to copper(I), starting from $[(CH_3CN)_4Cu^I(BF_4)]$ and two equivalents of (*R*)-BOX-Ind, we isolated the homoleptic ML_2 complex $[Cu^I\{(R)\text{-BOX-Ind}\}_2][BF_4]$ (**5**)

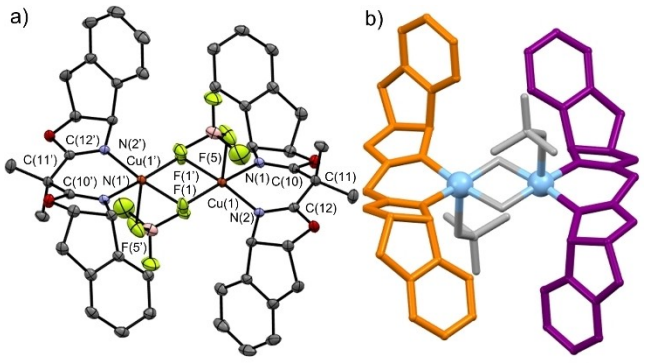

Figure 5. Molecular structure of $[(BOX\text{-}Ind)Cu^{II}F]_2[BF_4]_2$ (4): a) ORTEP view. Hydrogens are omitted for clarity. Selected bond lengths (Å) and angles (°): Cu(1)–N(1) 1.9785(13); Cu(1)–N(2) 1.9615(13); Cu(1)–F(1) 1.9207(11); Cu(1)–F-(5) 2.455(11); Cu–Cu 2.9391(4). (b) Molecular structure of the complex with (*R*)-BOX-Ind in orange and (*S*)-BOX-Ind in violet (methyl groups are omitted for clarity).

in 75% yield, as deduced from mass spectrometry, elemental analysis and NMR analysis (eq. 5). ^{1}H-NMR analysis showed a upfield shift of the C–*H* oxazoline signals in comparison to the free bisoxazoline ligand (Figure S4). Despite several crystallization attempts, no crystal suitable for X-ray analysis has been obtained for compound (**5**). The chiroptical properties of the homoleptic copper(I) complex were measured, however only a weak signal was recorded.

$$\underset{\textit{enantiopure}}{2\ BOX\text{-}Ind + [(CH_3CN)_4Cu^I(BF_4)]} \longrightarrow \underset{\textit{homochiral}}{[Cu(BOX\text{-}Ind)_2]^+} \quad (5)$$

By carrying out the same reaction but starting with the racemic ligand, the corresponding ML_2 $[Cu^I(BOX\text{-}Ind)_2][BF_4]$ (**6**) complex was isolated in 85% yield as colourless needles (eq. 6). The analysis by X-ray diffraction revealed that the complex is heterochiral, as displayed in Figure 6. Indeed, helped by the tetrahedral geometry of Cu^I centre, the metal is surrounded by

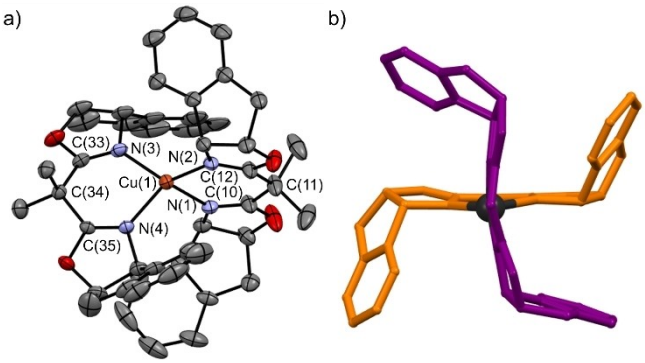

Figure 6. Molecular structure of heterochiral $[Cu^I(BOX\text{-}Ind)_2][BF_4]$ (6): a) ORTEP view. Hydrogens are omitted for clarity. Selected bond lengths (Å) and angles (°): Cu(1)–N(1) 2.064(2); Cu(1)–N(2) 2.002(3); Cu(1)–N(3) 2.002(3); Cu(1)–N(4) 2.050(2); N(1)–Cu(1)–N(2) 91.04(10); N(3)–Cu(1)–N(4) 90.96(10); N(2)–Cu(1)–N(3) 129.71(10); N(2)–Cu(1)–N(4) 117.86(10); N(1)–Cu(1)-N(3) 118.19(10); N(1)–Cu(1)–N(4) 110.02(10). (b) Molecular structure of the complex with (*R*)-BOX-Ind in orange and (*S*)-BOX-Ind in violet (methyl groups are omitted for clarity).

Research Article
doi.org/10.1002/ejic.202400527

two enantiomers of opposite chirality, forming a heteroleptic complex. It has a distorted tetrahedral geometry ($\tau_4 = 0.80$). Cu–N bond lengths are in the range of related complexes.[11,12,14–17] The ^{1}H NMR spectrum of the heterochiral Cu^I complex (**6**) shows that the two protons in positions C3 and C4 of the oxazoline are strongly shifted in the high field due to the proximity of the benzene ring of the opposite ligand, which is not the case for the homochiral species (Figure S4).

$$\underset{\textit{racemic}}{2\ \text{BOX-Ind}} + [(CH_3CN)_4Cu^I(BF_4)] \longrightarrow \underset{\textit{heterochiral}}{[Cu^I(\text{BOX-Ind})_2]^+} \quad (6)$$

Coordination Chemistry with BOX-Ph Ligands

We finally turned our attention to the BOX-Ph ligand. Homochiral copper(II) was obtained in 89% yield as a green crystalline solid starting from enantiopure (*R*)-BOX-Ph or (*S*)-BOX-Ph (eq. 7). Figures 7a and b displays the molecular structure obtained from (*S*) ligand. The copper centre has a highly distorted square planar geometry ($\tau_4 = 0.53$), as already observed in the molecular structure of the homoleptic complex (**3**) with BOX-Ind ligand. The two enantiomers were studied by CD (Figure 7c). They show an intense band peaking at 251 nm, two bands at 299 and 341 nm and an intense band at 660 nm which is characteristic to d-d transition bands.

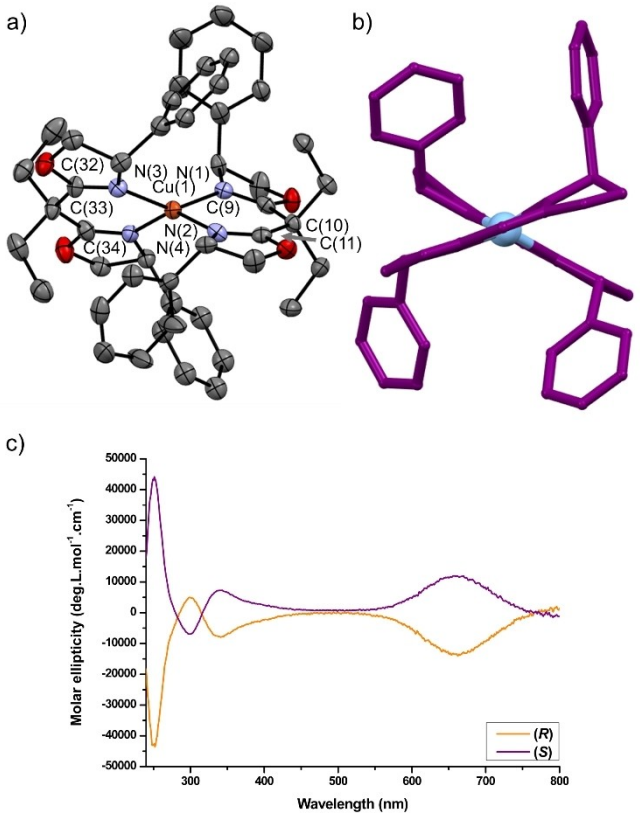

Figure 7. Molecular structure of $[Cu^{II}\{(S)\text{-(BOX-Ph)}\}_2][BF_4]_2$ (7): a) ORTEP view. Hydrogens and BF_4^- counter-ions are omitted for clarity. Selected bond lengths (Å) and angles (°): Cu(1)–N(1) 1.989(7); Cu(1)–N(2) 2.023(7); Cu(1)–N(3) 1.968(5); Cu(1)–N(4) 1.973(6); C(9)–N(1) 1.276(11); C(11)–N(2) 1.273(11); C(32)–N(3) 1.284 (9); C(34)–N(4) 1.285(9); N(1)–Cu(1)–N(2) 89.7(3); N(3)–Cu(1)–N(4) 91.9(2); N(1)–Cu(1)–N(4) 105.2(3); N(2)–Cu(1)–N(3) 96.5(3); N(2)–Cu(1)–N(4) 141.0(3); N(1)–Cu(1)–N(3) 144.0(3); C(9)–C(10)–C(11) 114.7(8); C(32)–C(33)–C(34) 112.5(6). (b) Molecular structure of the complex with (*S*)-BOX-Ph in violet (methyl groups are omitted for clarity); c) Circular dichroism (CD) of the two enantiomers of (7) ($c = 3.55.10^{-4}$ M in dichloromethane).

$$\underset{\textit{enantiopure}}{2\ \text{BOX-Ph}} + [Cu^{II}(BF_4)_2] \longrightarrow \underset{\textit{homochiral}}{[Cu^{II}(\text{BOX-Ph})_2]^{2+}} \quad (7)$$

Running the same reaction on a racemic mixture (eq. 8) of the ligand leads mostly to the formation of homochiral species, as deduced from X-ray crystallography (Figure S5), with the centrosymmetric space group $P2_1/C$. However, after careful refinement, the crystalline lattice revealed a disorder that shows the presence of the heterochiral species, a situation also recently encountered by Kleij, Maseras *et al.* with related complexes (Figure S6).[12] Therefore, the measured crystal was shown to be a mixture of 40% homochiral (*R*), 40% homochiral (*S*) and 20% heterochiral. In all cases, the molecular structures show fairly similar spatial arrangements, in particular the phenyl group of one ligand is positioned orthogonally to the opposite ligand in a very long CH-π interaction (2.8–3.8 Å).

$$\underset{\textit{racemic}}{2\ \text{BOX-Ph}} + [Cu^{II}(BF_4)_2] \longrightarrow \begin{array}{c}[Cu^{II}(\text{BOX-Ph})_2]^{2+}\\ \textit{homochiral}\ (80\%)\\ +\\ \textit{heterochiral}\ (20\%)\end{array} \quad (8)$$

Intrigued by the possibility of having both homo and hetero forms, in an additional experiment, we set out to study the behavior of two different BOX-Ph ligands of opposite chirality but bearing different substituents on the bridging carbon of the ligand ((*R*)-BOX-Me, Me–Ph and (*S*)-BOX-Bn, Me–Ph) (eq. 9). This could lead to the formation of two different homochiral complexes, or alternatively to the unique formation of a single heterochiral species of lower symmetry. Here, a single complex was formed in 74% isolated yield and all analyses are consistent with the formation of the heterotopic copper(II) complex (**7′**) $[Cu^{II}\{(S)\text{-BOX-Bn, Me–Ph}\}\{(R)\text{-BOX-Me, Me–Ph}\}][BF_4]_2$, which was confirmed by X-ray diffraction studies (Fig. 8). The metal adopts a distorted tetrahedral geometry ($t_4 = 0.67$), which is very unusual for copper(II).[18] Cu–N bond lengths range from 1.946(5) Å to 1.989(4) Å, corresponding to the classic ranges for this type of compound.[11,12,14–17] Interestingly, the structure displays CH-π interligand interactions between the phenyl rings and the C4 hydrogen of the oxazoline (distances measured between the phenyl centroid and the H ranging from 2.47 Å and 2.74 Å), which could favour the thermodynamic stability of the complex.

Research Article
doi.org/10.1002/ejic.202400527

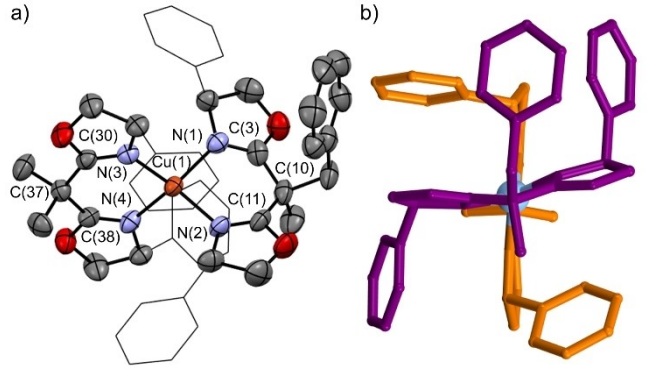

Figure 8. Molecular structure of the heterotopic complex [Cu^{II}{(*S*)-BOX-Bn, Me–Ph}{(*R*)-BOX-Me, Me–Ph}][BF_4]$_2$ (7′): a) ORTEP view. Hydrogens and BF_4^- counter-ion are omitted for clarity. Selected bond lengths (Å) and angles (°): Cu–N(1) 1.983(5); Cu–N(2) 1.989(4); Cu–N(3) 1.955(4); Cu–N(4) 1.946(5); N(1)–Cu–N(2) 91.6(2); N(3)–Cu–N(4) 91.26(18); N(1)–Cu–N(4) 133.92(19); N(2)–Cu–N(3) 131.69(19); N(2)–Cu–N(4) 107.3(2); N(1)–Cu–N(3) 107.01(19). (b) Molecular structure of the complex (7′) with (*R*)-BOX-Me, Me–Ph in orange and (*S*)-BOX-Bn, Me–Ph in violet.

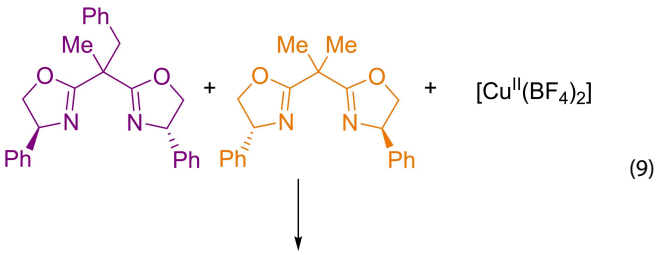

(9)

[Cu^{II}{(*S*)-BOX-Bn,Me-Ph}{(*R*)-BOX-Me,Me-Ph}][BF_4]$_2$ (**7'**)

Finally, the coordination chemistry of BOX-Ph was studied with copper(I) and the results show the same behavior as for the BOX-Ind ligand, namely the formation of a homochiral complex [Cu^{I}{(*S*)-BOX-Ph}$_2$][BF_4] (**8**) (eq. 10) in the presence of the enantiopure ligand (74% yield) and the formation of a heterochiral complex [Cu^{I}(BOX-Ph)$_2$][BF_4] (**9**) (eq. 11) in the presence of the racemic ligand (83% yield). Figure 9 displays the two molecular structure as deduced from X-ray diffraction studies. These results were also confirmed by means of NMR spectroscopy (Figure S7).

2 BOX-Ph + [$(CH_3CN)_4Cu^{I}(BF_4)$] ⟶ [Cu^{I}(BOX-Ph)$_2$]$^+$
enantiopure *homochiral* (10)

2 BOX-Ph + [$(CH_3CN)_4Cu^{I}(BF_4)$] ⟶ [Cu^{I}(BOX-Ph)$_2$]$^+$
racemic *heterochiral* (11)

Dynamic Behaviour: Homochiral/Heterochiral Interconversion

On the basis of these results obtained by solid-state X-ray diffraction studies, which show that the oxazoline substituents behave differently, we studied the stability of these compounds in solution. Self-recognition or self-discrimination in these systems could be triggered electrochemically by changing the oxidation state of the Cu atom, which can be usefully studied by cyclic voltammetry.[6,7]

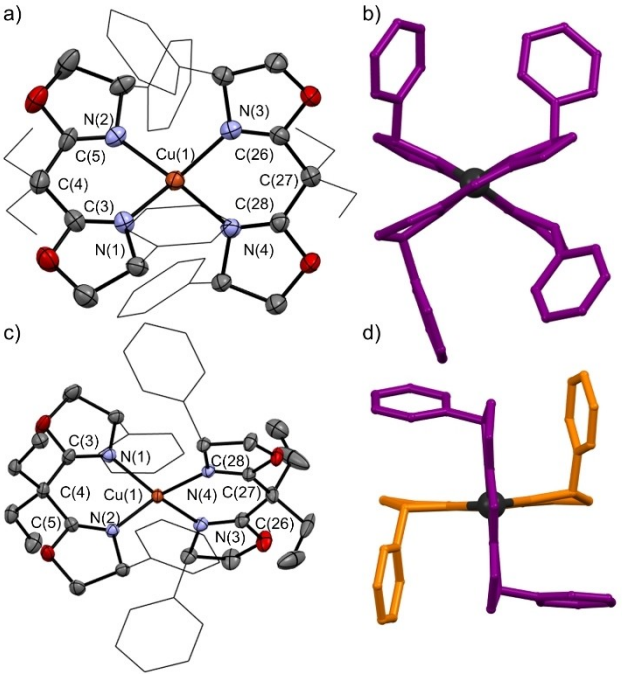

Figure 9. a) Molecular structure of the homoleptic complex [Cu^{I}{(*S*)-BOX-Ph}$_2$][BF_4] (8): ORTEP view. Hydrogens, ethyl groups and BF_4^- counter-ion are omitted for clarity. Selected bond lengths (Å) and angles (°): Cu–N(1) 2.047(4); Cu–N(2) 2.034(4); Cu–N(3) 2.052(4); Cu–N(4) 2.039(5); N(1)–Cu–N(2) 90.34(18); N(3)–Cu–N(4) 90.68(18); N(2)–Cu–N(4) 137.46(17); N(1)–Cu–N(4) 109.85(18); N(2)–Cu–N(3) 106.82(18); N(1)–Cu–N(3) 126.98(17); C(3)–C(4)–C(5) 114.1(5); C(26)–C(27)–C(28) 114.4(4). b) Molecular structure of the complex (8) with (*S*)-BOX-Ph in violet. c) Molecular structure of the heteroleptic complex [Cu^{I}(BOX-Ph)$_2$][BF_4] (9): ORTEP view. Hydrogens, ethyl groups and BF_4^- counter-ion are omitted. Selected bond lengths (Å) and angles (°): Cu–N(1) 2.0365(16); Cu–N(2) 2.0357(15); Cu–N(3) 2.0294(16); Cu–N(4) 2.0357(15); N(1)–Cu–N(2) 88.40(6); N(3)–Cu–N(4) 88.45(6); N-(2)–Cu–N(4) 117.63(6); N(1)–Cu–N(4) 118.78(6); N(2)–Cu–N(3) 122.52(6); N(1)–Cu–N(3) 124.43(6); C(3)–C(4)–C(5) 113.33(15); C(26)–C(27)–C(28) 113.16(15). d) Molecular structure of the complex (9) with (*R*)-BOX-Ph in orange and (*S*)-BOX-Ph in violet (ethyl groups are omitted for clarity).

Figure 10 displays the cyclic voltammograms (CVs) using the enantiopure or the racemic ligands recorded at a potential sweep rate of 100 mV s^{-1}. With BOX-Bn ligand (Figure 10a), starting from a positive potential, a reduction wave denoted as $\mathbf{c_1}$ is observed at +0.02 V vs Fc^+/Fc and, upon the reverse scan, the reversible oxidation wave is observed as $\mathbf{a_1}$ at +0.15 V. We also observed $\mathbf{a_2}$/$\mathbf{c_2}$ redox peak at $E_{1/2}$ = −0.30 V with a significantly lower intensity than the $\mathbf{a_1}$/$\mathbf{c_1}$ redox peak. The same experiment carried out with the racemic ligand did not alter the overall voltammogram. On the basis of these redox potential values and in particular in comparison with the results obtained with the following other systems, as an attempt to assign signals, the reversible signal $\mathbf{a_1}$/$\mathbf{c_1}$ could correspond to the homochiral ML_2 species. This hypothesis is reinforced by the isolation of species that are homochiral with copper(I), whatever the enantioselectivity of the ligand. The monoligated copper(II) complex [(BOX-Bn)Cu^{II}F(H_2O)][BF_4] (**1**) could be favoured in the solid state, during the slow crystallisation process.

Research Article
doi.org/10.1002/ejic.202400527

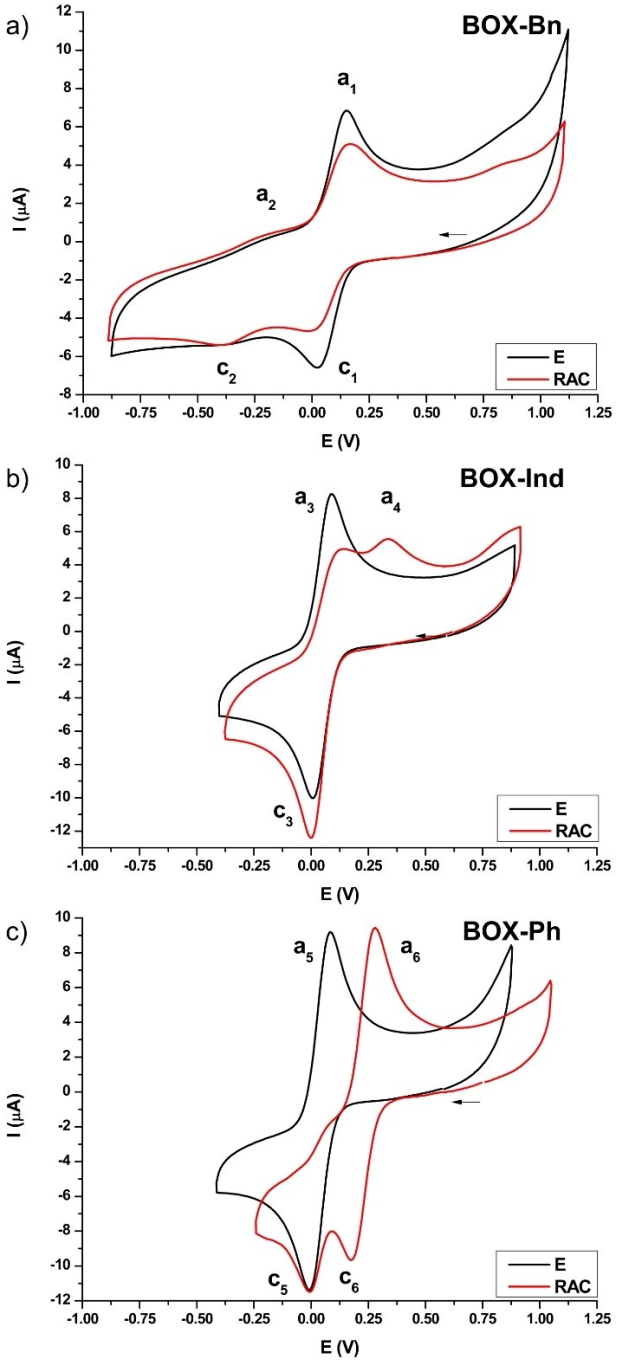

Figure 10. Cyclic voltammograms of a) the enantiopure mixture of (*S*)-BOX-Bn with $[Cu^{II}(BF_4)_2]$ (ratio 2 : 1) (black curve) and of the corresponding racemic mixture (ratio 1 : 1 : 1) (red curve), b) the enantiopure mixture of (*S*)-BOX-Ind with $[Cu^{II}(BF_4)_2]$ (ratio 2 : 1) (black curve) and of the corresponding racemic mixture (ratio 1 : 1 : 1) (red curve), and c) the enantiopure mixture of (*S*)-BOX-Ph with $[Cu^{II}(BF_4)_2]$ (ratio 2 : 1) (black curve) and of the corresponding racemic mixture (ratio 1 : 1 : 1) (red curve), on a glassy carbon electrode at a concentration of ca. 1 mM in 0.1 M $TBAPF_6$, in a dichloromethane solution. Scan rate 100 mV s^{-1}. The potential axis is referred to the Fc^+/Fc redox potential.

The cyclic voltammogram with the BOX-Ind ligand is different (Figure 10b). The black curve shows the CV of the homochiral enantiopure complex $[Cu^{II}\{(R)\text{-(BOX-Ind)}\}_2]^{2+}$ (**3**). Starting from a positive potential, the reduction wave of (**3**) into $[Cu((R)\text{-BOX-Ind})_2]^+$ (**5**) is observed at *ca.* 0 V vs Fc+/Fc ($\mathbf{c_3}$). Upon the reverse scan, the generated (**5**) is oxidized at *ca.* +0.09 V ($\mathbf{a_3}$). The Cu^{II}/Cu^{I} redox transition is reversible and similar features are obtained for the CVs of the (*S*) enantiomer.

Next, the reduction wave of the racemic mixture of BOX-Ind occurs at the same potential and with approximately the same intensity as for the homochiral enantiopure Cu^{II} complexes (Figure 10b, c3, red curve) and, during the backward scan, two oxidation waves, separated by 250 mV, are observed. The first oxidation wave $\mathbf{a_3}$, at ca. 0.09 V corresponds to the oxidation of the metastable homochiral Cu^{I} complexes (**5**). The second oxidation wave, denoted as $\mathbf{a_4}$, at a higher potential (*i.e.*, +0.34 V) is attributed to the more stable heterochiral $[Cu^{I}(BOX\text{-}Ind)_2]^+$ (**6**), resulting from the homochiral/heterochiral interconversion triggered by the reduction of Cu^{II} into Cu^{I}. Overall, this system behaves in a similar way to that previously observed with the BOX-*i*Pr ligand.[3,6,7] Since homochiral Cu^{II} species is the product of both anodic waves $\mathbf{a_3}$ and $\mathbf{a_4}$, the difference in their redox potential can be ascribed to the increased stability of the heterochiral Cu^{I} compared to the homochiral Cu^{I} complex by approximately −24 kJ/mol.

Finally, Figure 10c displays the CVs with the BOX-Ph ligand. The voltammogram with the enantiopure complex (black curve) is similar to the one obtained from BOX-Ind, i.e. a reversible Cu^{II}/Cu^{I} redox transition with $\mathbf{a_5}/\mathbf{c_5}$ values of −0.01 V and +0.08 V, respectively. On the other hand, the situation with the racemic BOX-Ph ligand is also different from the two previous cases. Starting from a positive potential, two reduction waves are observed (red curve), including the wave for the reduction of the homochiral species labeled as $\mathbf{c_5}$. The first reduction wave present at higher voltage ($\mathbf{c_6}$, +0.17 V) is a signature of the Cu^{II} heterochiral complex, while the second reduction at −0.01 V is due to the Cu^{II} homochiral complex. In the backward scan, the oxidation wave of the homochiral Cu^{I} complex $\mathbf{a_5}$ has very weak in intensity and a second oxidation wave, denoted as $\mathbf{a_6}$, at a higher potential (*i.e.*, +0.26 V) consistent with the formation of more stable Cu^{I} heterochiral species $[Cu^{I}(BOX\text{-}Ph)_2]^+$. According to the redox potential values, a redox reaction between Cu^{II} heterochiral complex and Cu^{I} homochiral is thermodynamically possible according ot the equation: Cu^{II} heterochiral + Cu^{I} homochiral → Cu^{II} homochiral + Cu^{I} heterochiral. Thus, the low intensity of the $\mathbf{a_5}$ peak might be also attributed to the consumption of the Cu^{I} homochiral species generated at the electrode surface through a reaction with Cu^{II} heterochiral complex present in the bulk of the solution. This study clearly demonstrates that homochiral and heterochiral copper(II) complexes can coexist in solution with BOX-Ph, exactly as in the solid state.

Conclusions

In conclusion, the complete series of homoleptic copper(I) and copper(II) complexes stabilized by chiral bisoxazoline ligands containing benzyl, indanyl or phenyl moieties has been synthesized, characterized and also studied in solution using cyclic voltammetry, highlighting the uniqueness of each system.

Research Article
doi.org/10.1002/ejic.202400527

We have found that the size of the substituents on chiral ligands is not the only parameter that needs to consider to control the heteroformation or homoformation of homoleptic complexes. The flexibility/rigidity of the systems and the possibility of weak interactions between the ligands contribute to the differences observed between the three systems. The results obtained with BOX-Ph ligand were the most surprising, with the phenyl substituents stabilizing both homochiral and heterochiral copper(II) Td species. It should be noted that the BOX-Ph ligand has been observed to induce a reversal of enantioselectivity in many cases in the context of asymmetric catalysis, thus underlining its distinctive features.[15,19] These features could be utilized in the future to develop sophisticated metallo-supramolecular systems that can be stimulated by redox processes.

Acknowledgements

We thank Corinne Bailly and Dr. Nathalie Gruber (University of Strasbourg) for the X-ray structural determinations and Emilie Couzigné and Emilie Voirin for technical assistance. We also thanks Dr. Martine Heinrich and Noémie Schneider from the University of Strasbourg and Jean-marc Strub from the IPHC analytic platform for the CD and mass spectroscopy measurements. This work was supported by IdEx Unistra (ANR 10 IDEX 0002), and by SFRI STRAT'US project (ANR 20 SFRI 0012) and EUR QMAT ANR-17-EURE-0024 under the framework of the French Investments for the Future Program. We also would like to thank the Région Grand Est for its partial financial support.

Conflict of Interests

The authors declare no conflict of interest.

Data Availability Statement

The data that support the findings of this study are available from the corresponding author upon reasonable request.

Keywords: Bisoxazoline · Bisimidazoline · Coordination chemistry · Chirality

[1] M. R. Taylor, E. J. Simon, J. Dickey, K. A. Hogan, N. A. Campbell, *Campbell Biology: Concepts & Connections*, Pearson, New York, NY **2021**.
[2] M. Torres, B. Heinrich, K. Miqueu, S. Bellemin-Laponnaz, *Eur. J. Inorg. Chem.* **2012**, *2012*, 3384–3387.
[3] M. Marinova, M. Torres-Werlé, G. Taupier, A. Maisse-François, T. Achard, A. Boeglin, K. D. "Honorat" Dorkenoo, S. Bellemin-Laponnaz, *ACS Omega* **2019**, *4*, 2676–2683; Dorkenoo, S. Bellemin-Laponnaz, *ACS Omega* **2019**, *4*, 2676–2683.
[4] J. M. Takacs, P. M. Hrvatin, J. M. Atkins, D. S. Reddy, J. L. Clark, *New J. Chem.* **2005**, *29*, 263–265.
[5] J. M. Atkins, S. A. Moteki, S. G. DiMagno, J. M. Takacs, *Org. Lett.* **2006**, *8*, 2759–2762.
[6] M. Marinova, A. Bonnefont, T. Achard, A. Maisse-François, S. Bellemin-Laponnaz, *Chem. Commun.* **2020**, *56*, 8703–8706.
[7] M. Marinova, A. Bonnefont, T. Achard, A. Maisse-François, S. Bellemin-Laponnaz, *Chirality* **2021**, *33*, 602–609.
[8] L. Gimeno, B. T. Phelan, E. A. Sprague-Klein, T. Roisnel, E. Blart, C. Gourlaouen, L. X. Chen, Y. Pellegrin, *Inorg. Chem.* **2022**, *61*, 7296–7307.
[9] C. Queffélec, P. B. Pati, Y. Pellegrin, *Chem. Rev.* **2024**, *124*, 6700–6902.
[10] S. Dagorne, S. Bellemin-Laponnaz, A. Maisse-François, *Eur. J. Inorg. Chem.* **2007**, *2007*, 913–925.
[11] G. Desimoni, G. Faita, K. A. Jørgensen, *Chem. Rev.* **2011**, *111*, PR284–PR437.
[12] A. Garcia-Roca, R. Pérez-Soto, G. Stoica, J. Benet-Buchholz, F. Maseras, A. W. Kleij, *J. Am. Chem. Soc.* **2023**, *145*, 6442–6452.
[13] L. Yang, D. R. Powell, R. P. Houser, *Dalton Trans.* **2007**, *9*, 955–964.
[14] P. Segl'a, M. Koman, T. Glowiak, *J. Coord. Chem.* **2000**, *50*, 105–117.
[15] J. Thorhauge, M. Roberson, R. Hazell, J. Jorgensen, *Chem. Eur. J.* **2002**, *8*, 1888.
[16] Y.-M. Zhang, L. Xian, T.-B. Wei, K.-B. Yu, *J. Chem. Res.* **2003**, *12*, 798–799.
[17] K. Matsumoto, K. Jitsukawa, H. Masuda, *Tetrahedron Lett.* **2005**, *46*, 5687–5690.
[18] N. Kitajima, K. Fujisawa, Y. Morooka, *J. Am. Chem. Soc.* **1990**, *112*, 3210–3212.
[19] D. A. Evans, J. S. Johnson, E. J. Olhava, *J. Am. Chem. Soc.* **2000**, *122*, 1635–1649.

Manuscript received: August 13, 2024
Revised manuscript received: September 4, 2024
Accepted manuscript online: September 6, 2024
Version of record online: October 29, 2024